REVISION 1

AIM analysis and the form of the bond-valence equation

Matthew C. F. Wander, Barry R. Bickmore, Larissa Lind, Charles Andros, John Hunt, Hannah Checketts, and Tyler Goodell

Department of Geological Sciences, Brigham Young University, Provo, UT 84602, U.S.A. E-mail: mcfwander@gmail.com

Abstract

The bond-valence model (BVM) posits an inverse relationship between bond valence (essentially bond order) and bond length, typically described by either exponential or power-law equations. To assess the value of these forms for describing a wider range of bond lengths than found in crystals, we first assume that the bond critical point density (ρ_b, reported in $e^-/Å^3$) is at least roughly proportional to bond valence. We then calculate ρ_b-distance curves for a number of diatomic pairs using electronic structure calculations (CCSD/aug-cc-pVQZ) and Atoms-In-Molecules (AIM) analysis. The shapes of these curves cannot be completely described by the standard exponential and power-law forms, but are well described by a three-parameter hybrid of the exponential and power-law forms. The ρ_b-distance curves for covalent bonds tend to exhibit exponential behavior, while metallic bonds exhibit power-law behavior, and ionic bonds tend to exhibit a combination of the two. We next use a suite of both experimental and calculated (B3LYP/Def2-TZVP) molecular structures of oxo-molecules, for which we could infer X-O bond valences of ~1.0 v.u. or ~2.0 v.u., combined with some crystal structure data, to estimate the curvature of the bond valence-length relationship in the high-valence region. Consistent with the results for the ρ_b-distance curves, the standard forms of the bond valence-length equation become inadequate to describe high-valence bonds as they become more ionic. However,

some of these systems demonstrate even higher curvature changes than our three-parameter hybrid form can manage. Therefore, we introduce a four-parameter hybrid form, and discuss possible reasons for the severe curvature. Although the addition of more parameters to the bond valence-length equation comes at a cost in terms of model simplicity and ease of optimization, they will be necessary to make the BVM useful for molecular systems and transition states.

Introduction

The bond-valence model (BVM) is a simple, empirical bonding model, notable for its ability to predict favorable combinations of bond lengths in complex condensed-phase structures, including both solids and liquids (Brown, 2002; Bickmore et al., 2009; Brown, 2009). It has, for the most part, been developed within the framework of the ionic (Madelung) bonding model, using electric flux lines between ions as the physical basis for bond valence. Non-ionic effects on bond length are largely incorporated through empirical calibration of separate bond-valence parameters for different cation-anion pairs (Brown, 1981; Preiser et al., 1999; Brown, 2002; 2013).

The fact that the BVM is at least in some respects conceptually unrealistic could be seen as a point in its favor, because such models are often the most useful, at least within their limited domains of applicability (Cotton, 1964). If we plan to expand the domain of applicability, however, it should be done with reference to more fundamental theory, i.e., quantum mechanics. Taken by itself, the BVM does not have any fundamental basis in quantum mechanics. However, some have developed links to quantum mechanics on the basis of similar predictions of chemical behavior. Burdett and Hawthorne (1993), for instance, related key aspects of the BVM to molecular orbital theory. Gibbs has long argued for using Bader's Atoms in Molecules (AIM) theory as a basis for rationalizing the BVM (Gibbs et al., 2001; Gibbs et al., 2014).

One possible area for expansion of the BVM is to incorporate bond-valence terms into molecular mechanics potential energy models. This has already been done (Adams and Swenson, 2002; Grinberg et al., 2002; Cooper et al., 2003; Shin et al., 2005; Adams and Rao, 2009; Grinberg et al., 2009; Liu et al., 2013a; Liu et al., 2013b), using bond-valence

parameters calibrated on crystal structures. The range of bond lengths for a given cation-anion pair, however, is limited in crystals, so it is questionable whether bond-valence-bond-length curves calibrated on crystals accurately cover the wide range of bond lengths one might expect to encounter in a molecular dynamics simulation, or even in gas-phase molecules (Brown, 2002; 2009).

Two main types of bond valence-length relationships have been proposed: exponential and power-law forms. But it is unclear whether one would outperform the other over a broader range of bond lengths. As noted above, one approach to addressing issues such as this is to draw inspiration from demonstrated links between the BVM and quantum mechanics. One promising avenue is the Quantum Theory of Atoms in Molecules (QTAIM or AIM) of Bader (Bader, 1991; Popelier, 2000), which provides an intriguing method for reducing the complex electron density distributions in molecules and crystals to a manageable set of descriptors that have been shown to be quite useful for rationalizing chemical structure and reactivity. Gibbs and coworkers (Gibbs et al., 2001; Gibbs et al., 2003; Gibbs et al., 2004; Gibbs et al., 2006; Gibbs et al., 2008a; Gibbs et al., 2008b; Gibbs et al., 2014) have demonstrated a strong correlation between bond valence and one of the primary AIM descriptors, the bond critical point electron density, in oxide crystals and some analogous molecules. If so, this suggests that one could use this relationship by way of analogy to generate hypotheses about the proper form of the bond valence-length relationship. Here we show how this can be done, by performing electronic structure calculations on molecules, and AIM analysis of the electron density.

Theory

The Bond-Valence Model

Bond valence can be thought of as essentially the same thing as bond order, i.e., the number of valence electron pairs involved in a bond (Brown, 2002). The difference between this and other bond-order schemes is that bond valence is related solely to inter-nuclear distance, rather than more complex quantities like bond overlap populations, and bond valence-length curves are empirically calibrated to conform to a certain criterion, called the valence sum rule. Equations 1 and 2 are two forms of the equation relating the valence of a bond between ions *i* and *j* (s_{ij}) to the bond length (R). In both cases, R_0 is the length of a bond with a valence of 1.0 valence units (v.u.), and B is a "softness" parameter that governs the curvature of the relationship. The value of s_{ij} is taken to be positive in the direction from cation to anion.

$$\left|s_{ij}\right| = e^{(R_0 - R)/B} \quad (1)$$

$$\left|s_{ij}\right| = (R/R_0)^{-1/B} \quad (2)$$

Bond-valence parameters (R_0 and B) for individual ion pairs are generally calibrated on numerous empirically determined crystal structures by enforcing the valence sum rule (Eqn. 3), which requires that the valence sum of bonds incident to an ion *i* from counter-ions *j* is equal to negative the atomic valence (V_i), i.e., the formal charge, of ion *i*.

$$\sum_j s_{ij} + V_i = 0 \quad (3)$$

The empirical calibration is a very important feature of the model, because it implicitly rolls in effects on bond length other than those related to bond order, such as Van der Waals interactions (Brown, 2002). The BVM has, therefore, been very successful at predicting favorable combinations of bond lengths for bonds incident to individual atoms (Brown, 2002). However, this also places an important limitation on our ability to exactly

relate bond valence to quantities derived from quantum mechanics, such as bond critical point densities.

The exponential form of the bond-valence equation (Eqn. 1) is equivalent to the bond-order equation proposed by Pauling (1947), whereas two power-law forms essentially equivalent to Eqn. 2 were proposed by Brown and Shannon (1973). It should be emphasized that the two forms cannot be made exactly equivalent by allowing for different R_0 and B values. If these equations are calibrated on crystal structures and applied to crystal structures, it probably matters little which form of the equation is used, because crystals exhibit a limited range of bond lengths for a given ion pair, and either form could be fit well to the data over such a limited range. However, if one intends to use a bond-valence equation over a broader range of bond lengths, including shorter bonds found in molecules and transition states, as well as longer, secondary bonds, the form of the equation may become important (Brown, 2002; 2009). Here we explore the possibility of using AIM theory to inform the process.

Atoms in Molecules and the BVM

AIM is fundamentally a method for describing the total electron density distribution (ρ), which is a quantum mechanical observable, in molecules and crystals in a way that is useful for making connections with molecular structure and reactivity (Bader, 1991; Popelier, 2000). It defines chemical bonds and boundaries between atoms in terms of the critical points in the shape of the total electron density. These partitions can represent atoms or bonds or other aspects of the molecular structure. The critical points in the surface are all points where $\nabla\rho = 0$; e.g., maxima, minima, or saddle points. Certain saddle points are called bond critical points (BCPs), because they have two negative directions of

curvature and one positive, and are usually located near a straight line axis between two atoms. Bonds are described by the features of the electron density around BCPs, e.g., the bond critical point density (ρ_b) and the ellipticity (ϵ) of ρ in the vicinity. By defining atoms and bonds in terms of these key features in the electron density, AIM provides a simple mechanism for extracting information from a quantum mechanical wave function. Although AIM provides a fairly high-level (i.e., fundamental) view of molecular structure, some have attempted to relate AIM-derived quantities, such as ρ_b, to lower-level concepts more familiar to chemists. For instance, some (Bader et al., 1982; Popelier, 2000; Firme et al., 2009) have proposed an exponential relationship between bond order and ρ_b.

Recently, some relevant work has been published relating AIM descriptors to bond order in a more complex manner (Matta, 2014). These have used ρ_b, $\nabla^2\rho_b$ (the Laplacian of ρ_b), and bond ellipticity to relate bond order to the bond length, or a newer quantity called the delocalization index (Matta, 2014). Here, the bond order is posited to be based on the delocalization matrix and is approximately equal to the count of the electrons at a bond critical point. This idea has been developed for the case of strong bonding (Matta and Hernández‐Trujillo, 2003), and has been explored thoroughly for H…H bonding, where a similar relationship was observed (Cukrowski and Matta, 2010). A similiar relationship has also been observed for biological molecules (Zhurova et al., 2006). Finally, an examination of extremely short bonds, featuring an interesting case of strong Ti-C bonds, was undertaken, in which a deviation from the expected monotonic increase was observed, (Zhurova et al., 2006).

Such relationships raise the possibility of a close correspondence between AIM descriptors and bond valence. The definition of a chemical bond varies between different

models, so direct comparisons are often problematic (Rzepa, 2009), e.g., between models that define bonds based on counting electron pairs or an inverse strength-distance relationship. Gibbs *et al*. (2014), however, surveyed s_{ij} and ρ_b in a number of oxide minerals and molecular analogues, and observed the relationship shown in Eqn.4, where $R_{M\text{-}O}$ is the metal-oxygen bond length, $s_{M\text{-}O}$ is the Pauling bond strength (i.e. an averaged bond valence calculated by dividing the atomic valence of the cation by its coordination number), and r is the row number of the element (taking the second row starting with Li as $r = 1$).

$$s_{M-O} \approx \rho_b = r\left(\frac{\rho_b}{R_{M-O}}\right)^{4.76} \quad (4)$$

On the one hand, the relationship in Eqn. 4 must be partially serendipitous, because the units used for ρ_b are $e^-/\text{Å}^3$, and a different choice of volume units would remove the 1:1 correspondence. Even an approximately linear relationship between the two seems significant, on the other hand, and should be further explored. Formally, bond order is about the nodal structure of the wavefunction. However, it seems reasonable to suppose that there would be a connection between the magnitude of ρ_b and various measures of bond order, because otherwise Density Functional Theory, and specifically the local density approximation, would not work.

There are reasons to expect some divergence between the BVM's s_{ij} value and AIM's ρ_b, however. First, calculation of ρ_b takes into account contributions of all atoms (via the Schrödinger Equation). This means that even if the positions of the two bonded atoms are not altered, alterations of the positions of other atoms will affect the calculated value of ρ_b (see Schema 1). In the BVM, however, bond valence is calculated solely on the basis of the

bond length between two atoms, and does not take into account the positions of any other atoms bonded to those two, or even whether there are any other bonded atoms.

Nevertheless, here we simply assume that ρ_b is at least roughly proportional to s_{ij}, the bond valence, and therefore the shapes of the ρ_b-distance curve for a given bond type should be similar to the s_{ij}-distance curve. Given this hypothesis, we can only draw tentative conclusions about the shapes of s_{ij}-distance curves, but we go on to devise an independent test of the hypothesis based on experimental and calculated molecular structures.

Methods

We generated ρ_b-distance curves via a series of electronic structure calculations on atom pairs from the first two rows of the periodic table, separated by variable distances, and performing AIM analysis. The electronic structure calculations were performed using Gaussian 09 (Frisch et al., 2010). All heterodiatomic and homodiatomic molecules from H to F (excluding He) were calculated at the CCSD/aug-cc-pVQZ level of theory. CCSD stands for coupled cluster theory with single and double excitations included, and the aug-cc-pVQZ basis set has four Gaussian functions per valence atomic orbital, and is specifically designed for coupled cluster calculations. The spin states used in the calculations are listed in Table S1 of the online supplement. The scans were from 0.5 Å to 4 Å in 0.5 Å increments, with an additional point at 6 Å. Most of the calculation parameters were set to defaults, but where possible, output wavefunctions were used as input for the next calculation in the series. Wavefunction (.wfn) files were generated for input into AIMAll (aim.tkgristmill.com) to identify the critical points in the structure and extract the electron density at those points (Keith, 2013) .

Our method of choice for the calculations was something of a guess. There is extremely limited benchmarking of the stability of electron densities. What has been published is at a much lower level of theory and showed that basis set size was at least as important as methodology (Jabłonski and Palusiak, 2010).

To test the hypothesis that s_{ij}-distance curves behave similarly to ρ_b-distance curves, we performed bond-valence analysis on the structures of a number of small oxo-molecules in which the bonds to the O atoms could be inferred to be close to single or double bonds. Experimental structures for these molecules were taken mainly from the NIST Computational Chemistry Comparison and Benchmark Database (http://cccbdb.nist.gov), and then supplemented with structures generated using hybrid density functional theory structure optimizations in Gaussian 09, at the B3LYP/Def2-TZVP level. The bond-valence analysis was performed using both exponential and power-law forms of the bond valence-length equation, using appropriate parameter sets calibrated on crystal structures (Brown and Shannon, 1973; Brown and Altermatt, 1985; Adams, 2001).

We also fit tentative bond-valence curves using the MATLAB curve-fitting toolbox. The code is available on request from B. R. Bickmore.

Results and Discussion

Table 1 shows the ρ_b-distance curves calculated for all the diatomic pairs. Attempts to fit these curves with exponential (Eqn. 1) and power-law (Eqn. 2) bond valence-length equations met with varying success, which we have illustrated using the curve for the LiF pair in Figure 1. The ρ_b-distance curve for LiF is shown in its normal (Fig. 1a) and log-linear (Fig. 1b) forms, along with best-fit exponential (Eqn. 1) and power-law (Eqn. 2) curves. On a log-linear plot the exponential function is linear, and the power function is

curved. This particular type of plot works well for illustrating the quality of the different fits at both long and short range. Neither form fits the data over the entire range, but either one would more adequately fit the data over a narrower range of bond lengths. (It should be noted that we fit logarithmic forms of Eqns. 1 and 2 to log(ρ_b) vs. distance, so as to more accurately capture the overall curvature at both long and short distances.)

Assuming ρ_b is roughly proportional to s_{ij}, it is apparent that a two-parameter exponential or power-law bond valence-length relationship is not sufficient over such a broad range of bond lengths. We have therefore explored hybrid models with more parameters. One such model is shown in Eqn. 5, created simply by taking a weighted geometric mean of the two forms (Eqns. 1-2). Here w is the weighting factor ($0 \leq w \leq 1$), equal to 1 when the curve is fully exponential, and 0 when is fully power-law.

$$\rho_b \propto \left|s_{ij}\right| = (R/R_0)^{-(1-w)/B} e^{(R_0-R)w/B} \qquad (5)$$

A best-fit three-parameter curve (Eqn. 5) is plotted with the LiF data in Figures 1a and 1b. One could also consider four and five parameter variants of Eqn. 5, first allowing the two B values to differ and then ultimately the two R_0 values. Each of these variants would provide a small additional increase in flexibility. The fit is nearly perfect over the entire scan, even outside of the range one could conceivably find real equilibrium bond lengths. Thus, such a curve might be accurate even for non-equilibrium structures sampled in molecular dynamics simulations, such as transition states, and long, secondary bonds.

We were able to obtain excellent fits of Eqn. 5 to all the ρ_b-distance curves. Table 2 shows the optimized model parameters (Eqns. 1, 2, and 5) for the full set of ρ_b scans. Table 3 breaks out the hybrid w values for both the Eqn. 5 fits to highlight trends related to bond type. Instead of ordering by atomic number, which would put H next to the metals, we

ordered in terms of Pauling electronegativity. The values form a triangular distribution with the most metallic bonds at one vertex, the most ionic bonds at another vertex, and the most covalent bonds at the third vertex, similar to the Ketelaar triangle (Ketelaar, 1958). (Note that we are referring to metal-metal bonds as "metallic" even in diatomic molecules, although we recognize that metallic properties require a more extended system.) This point is also illustrated by the contour plot shown in Figure 2a, where the shading indicates the w value for the Eqn. 5 fit, respectively, and the x- and y-axes (χ_1 and χ_2) represent the Pauling electronegativities of the two atoms (Allred, 1961). We see that, while both the exponential and power-law forms generally provide reasonably good fits, they are not equally good for all element pairs. Although the hybrid model (Eqn. 5) will obviously always provide the best fit, it is clear that the power-law form (Eqn. 2) is better than the exponential form (Eqn. 1) for metal-metal (metallic) bonds ($w < 0.5$ for the hybrid models), while the reverse is true for covalent bonds between nonmetals ($w > 0.5$). Ionic bonds have intermediate w values in the hybrid model, indicating that neither the exponential nor the power-law forms are preferred. Figure 2b shows a second-order polynomial fit to the w values based on χ_1 and χ_2, to highlight periodic trends. Figure 2c shows the w values predicted with the polynomial fits vs. those fitted to the ρ_b-distance curves, to illustrate the quality of the polynomial fits.

The periodic trends in the model parameters make good chemical sense. That is, they depend both on the character of the atoms (metal, metalloid, and nonmetal), and on the polarity of the bonds (non-polar covalent, polar-covalent, ionic). Metal atoms tend to have more depleted valence electron densities, but metallic bonds extend over a larger range, so metal-metal ρ_b values increase gradually as the bond length becomes shorter, but

then very rapidly at close range. This behavior would be more conducive to a power-law relationship (see Fig. 1). The opposite would be true of bonds between non-metals, and ionic bonds should show intermediate behavior.

There are two elements of particular interest, Boron and Fluorine. Boron seems to behave more as a metal when it is bound to a metal, and prefers more power character in the hybrid fit. When it is bound to a non-metal it behaves more like a non-metal and an exponential fit is preferred. When bound to itself, Boron prefers a more equal balance of power and exponential curvature, like ionic materials. The second element of interest is Fluorine, for which the *w* values dip slightly from the maximum of 1. We suspect this is a result of the high electron density around the fluorine, which will pack into anti-bonding orbitals, pushing the density outward. Finally, however, BF is an ionic bond (not polar covalent), so here Boron does not show its usual deferential quality.

Even supposing bond valence-length curves behave similarly, however, the bond lengths in our ρ_b-distance curves extend to as low as 0.5 Å, which is quite extreme for any type of bond. Given that adding a third or fourth parameter to the bond valence- length equation comes at a cost in terms of model simplicity, we need to show that such a model is needed to address the range of bond lengths one might actually find in real or calculated chemical systems. We can do that by using standard bond-valence calculations on simple molecules for which we can infer relatively accurate bond valences for strong bonds. For example, assuming the valence sum rule (Eqn. 3) applies, one could infer that the Si-O bonds in the disiloxane molecule, $(H_3Si)_2O$, or the Li-O bonds in the Li_2O molecule, are single bonds (~1 v.u.). Similarly, the M-O bonds in CO_2 or MgO are double bonds (~2 v.u.). Table 4 lists the bond lengths for a number of such molecules. All of these bonds should

have bond valences of either ~1 v.u., or ~2 v.u., but Table 4 also shows bond valences calculated for these bond lengths using Eqn. 1 (the exponential form) and R_0 and B parameters obtained from either Brown and Altermatt (1985), for which B is always set to 0.37 Å, or the SoftBV parameters of Adams (2001), for which B is a free parameter. Table 4 also shows bond valences calculated using two different power-law relationships and associated parameter sets proposed by Brown and Shannon (1973).

Figure 3 shows the deviation of the calculated bond valences from their inferred values (Δs_{ij}) plotted vs. the fraction ionic character of the bonds (I_b), obtained from Eqn. 7 (Pauling, 1960), where χ_1 and χ_2 are the Pauling electronegativities of the two atoms (Allred, 1961).

$$I_b = 1 - e^{-0.25(\chi_1 - \chi_2)^2} \quad (6)$$

Figs. 3a and b show the results for the exponential form (Eqn. 1), using the Brown and Altermatt (1985) and SoftBV (Adams, 2001) parameters, respectively. The plots clearly show that the inferred valences of more covalent single and double bonds tend to be calculated fairly accurately via the exponential bond-valence equation, but are systematically under-predicted as the bonds become more ionic. This is less the case for single-bond valences calculated with the Brown and Altermatt (1985) parameters, because a single "average" B value is assumed, and there both the most covalent and the most ionic bonds are under-predicted. Double bonds are systematically under-predicted as a function of ionicity for both parameter sets, however. Figures 6c and d show the results for two power-law forms proposed by Brown and Shannon (1973), one using parameters for individual cation-O pairs and the other with parameters that are universal for cations with the same number of core electrons, and both similar to Eqn. 2. Once again, both the single-

and double-bond valences are systematically under-predicted as a function of the bond ionicity.

These results were initially surprising because, while we expected the exponential form to underestimate the valences of the more ionic bonds, we also expected the power-law forms to overestimate the valences of the more covalent bonds (see Fig. 1). While it does turn out that the exponential form generally underestimates to a slightly greater degree, the reason for the observed behavior has more to do with the limited range of bond lengths available in calibration sets that include only crystals. Bonds of a given type in crystals tend to occur within a fairly narrow range around a certain expectation value. Brown and coworkers (Brown and Shannon, 1973; Brown, 1988; Brown and Skowron, 1990) estimated many of these expectation values for X-O bonds in oxides, called the "Lewis Acid Strength" ($L_{A,X}$) of each cation, by dividing each cation's atomic valence (V_X) by its average observed coordination number ($\overline{N}_c$) in a large set of oxide crystals (see Eqn. 7).

$$L_{A,X} = \frac{V_X}{\overline{N}_c} \qquad (7)$$

This value is highly correlated with the electronegativity of the cations, and therefore we expect that more ionic bonds will tend to have lower bond valences in crystals (see Eqn. 7). A consequence of this is that bond valence-length models for more ionic bonds, fit to calibration sets of crystal structures, would necessarily have to be extrapolated far outside the bond lengths found in crystals to reach 1-2 v.u. Meanwhile, the model parameters would be tailored to match the curvature of the valence-length relationship in the range found in crystals, which is typically not as strong in the low-valence region.

Figure 4 illustrates this point by plotting s_{ij} vs. bond length for four bond types involving Oxygen: Mg-O (I_b = 0.68), Be-O (I_b = 0.58), Si-O (I_b = 0.45), and Ge-O (I_b = 0.40).

These bond types were chosen because they cover a range of ionicity, single- and double-bond lengths were available in Table 4, both exponential and power-law bond-valence parameters were available, and $L_{A,X}$ estimates were also available (Brown, 1981; Brown and Skowron, 1990). For each bond type, we show points representing the ~1 and ~2 v.u. bond lengths from molecules in Table 4, another point representing $L_{A,X}$, with the corresponding bond length calculated via Eqn. 1 and Brown and Altermatt's (1985) parameter set, and two bond lengths from empirically determined crystal structures. The two crystals chosen for each bond type (see Table 5) had two different cation coordination numbers and very symmetrical cation coordination polyhedra (variations in bond lengths no more than a few hundredths of an Å). Thus, an average bond length could be accurately associated with the average bond valence (the cation valence divided by the coordination number. Figure 4 also shows for each bond type an exponential bond valence-length curve with parameters taken from Brown and Altermatt (1985), and a power-law curve with parameters taken from Brown and Shannon (1973). In all four cases, the exponential and power-law curves (both optimized on suites of crystal structures) are almost identical in the region around $L_{A,X}$ and the crystal values, but might differ significantly at much longer or shorter bond lengths.

As our example bonds become progressively more ionic, the curves become steeper and steeper in the high-valence (1-2 v.u.) region, consistent with our results for the ρ_b-distance curves. We optimized exponential (Eqn. 1), power-law (Eqn. 2), and three-parameter hybrid (Eqn. 5) models to fit the 1 and 2 v.u. points and the crystal values, but surprisingly, even Eqn. 5 was inadequate for the strong curvature needed to describe the more ionic bonds.

In addition, we have plotted in Figure 4 the optimized three-parameter hybrid (Eqn. 5) curves, as well as another curve representing the optimized four-parameter hybrid model in Eqn. 8. This is similar to Eqn. 5, except that it is a weighted arithmetic, rather than geometric, mean of the exponential (Eqn. 1) and power-law (Eqn. 2) forms, and separate softness parameters (B_{exp} and B_{pow}) are allowed for the two forms. The optimized parameter and misfit values for Eqn. 5 and Eqn. 8 are shown in Table 6. (It should be noted that the optimized *w* values in Table 6 are all zero for the Eqn. 5, but this merely reflects the fact that even a power-law function cannot match the high curvature exhibited by the data.)

$$\left|s_{ij}\right| = (1-w)(R/R_0)^{-1/B_{pow}} + we^{(R_0-R)/B_{exp}}, \quad (8)$$

Clearly, Eqn. 8 can produce the desired curvature, whereas Eqn. 5, or even a variant of Eqn. 8 with a single *B* parameter, cannot. Forms involving an arithmetic mean, similar to Eqn. 8, are uniformly more flexible than geometric means, given the same number of parameters. We conclude, therefore, that a more flexible curve shape than Eqns. 1-2, and even Eqn. 5, is very likely needed to describe bond valence-length relationships over the full range of bond lengths one might find in crystals, molecules, and transition states for certain element pairs. In fact, this problem can sometimes be detected even for the strongest bonds found in crystals for very ionic bond types. Bickmore et al. (2013), for instance, showed that while the alkali metal oxides (Li_2O, Na_2O, K_2O, and Rb_2O) all have 4-coordinated metals, and so should have X-O bond valences of only ~0.25 v.u., the SoftBV valence parameters (Adams, 2001) under-predict the valence sums on the ions by up to ~40-50% for the structures with the most ionic bonds (K_2O, and Rb_2O). This is the case even though the SoftBV parameters are specifically designed to have stronger interactions

at long distances, which should partially counterbalance underestimates of the high-valence bonds.

The severe curvature shown in Fig. 4 brings up a certain difficulty for our endeavor, however, if we want to develop the BVM to correctly predict things like bond dissociation energies and bond force constants (representing the stiffness of the bond at equilibrium). That is, for the most ionic bond type shown (Mg-O), the length of the nominal single bond (1.765 Å) is very close to that of the double bond (1.749 Å). Is it reasonable to suppose that the bond valence-length curve is so steep in this region that there can be a change of 1 v.u. over a distance of only a few hundredths of an Å? We drew this conclusion by simply assuming that the valence sum rule (Eqn. 3) is applicable to our suite of molecular structures, but this is not necessarily the case. By comparing bond dissociation energies in various compounds, for instance, Sanderson (1983) concluded that the bonds in the diatomic molecules of Group II oxides (including MgO) can only be single bonds, rather than double bonds, in effect making these molecules diradicals. He rationalized this by noting that the bonding orbitals about the Group 2a atoms (*sp* hybrids) are oriented opposite from one another, and therefore a double bond is geometrically impossible to form.

Given that the valence sum rule is the first axiom of the BVM, it seems reasonable to simply assume it, rather than arguing about whether an MgO bond is "really" a double bond, however. But if so, we still have to deal with the fact that in regions where there is abnormally high curvature in the bond valence-length curves, something different is probably occurring with respect to the relationship between bond valence and bond energy.

The likely culprit is changing bond character with bond length. Up to this point, we have used Pauling electronegativity differences to calculate the "fraction ionic character" of different bond types via Eqn. 6, which provides a single value for each bond type. However, it is well known that this is an oversimplification. Charge separation in most solids, for instance, decreases with increasing pressure (Batsanov and Batsanov, 2012); i.e., more compressed bonds in solids generally become more covalent, although there are some exceptions. It is also well known that, even given the same nominal bond order, bond energies can differ radically as a function of bond character, with more polar bonds heavily energetically favored (Pauling, 1960; Sanderson, 1983). Thus, if the change in charge separation for some types of bonds occurs more rapidly as the bonds are compressed in the high-valence (1-2 v.u.) region, becoming more covalent, it seems reasonable to suppose that the bond energy would change less rapidly with distance, leading to a smaller change in bond length for an equivalent change in bond valence.

This interpretation of increasing atomic charge makes sense from a quantum mechanical perspective. That is, an ion's charge is not located at a point at the center of mass but rather distributed over an approximately spherical volume. As two ions are brought together via a multiple bond, their electron clouds overlap to a much greater extent, reducing the partial charges on the individual ions. This pattern can be illustrated by the net dipoles of a series of hydrogenated molecules with C–O triple, double, and single bonds: C≡O (0.122D), H_2C=O (2.33D), and H_3C–OH (1.69D). At first glance, the lower dipole moment of the last molecule would seem to suggest lower charge separation, but the methanol net dipole is the result of the sum of two partially opposed CH_3–O and O–H dipole vectors, and actually indicates a much stronger separation of charge.

The specific format of Eqn. 8, with a single R_0 value but separate B values, dictates that the zone of rapid transition will be around 1 v.u. In fact, one could make an argument based molecular orbital theory that this is correct. Multiple bonds are characterized by a mixture of π and σ bonding, while single bonds and partial bonds are expected to exhibit purely σ character. As one distends a bond (in an equilibrium molecular configuration), from triple to double to single the π bonding is expected to fall off rapidly while the σ bonding is expected to be relatively unaffected. After a single bond is reached, the sigma bond diminishes proportionately (c.f., Haaland, 2008). This is clearly an oversimplification, but there is a transition that does occur in the electronic structure at just slightly above a single bond.

As mentioned above, however, adding a third or fourth parameter to the bond-valence equation comes at a cost in terms of model simplicity, and also ease of optimization. In fact, adequately constraining a three- or four-parameter curve such as Eqn. 5 would likely require data in at least four distinct bond length regimes, all with approximately determined bond orders. At minimum, one would need to augment calibration sets of crystal structures with molecular structures such as the ones employed here, and in some cases one would need alternative sources of information.

Utilizing established relationships between vibrational force constants and bond order (Johnston, 1966), along with periodic trends in vibrational force constants (Badger, 1934), seems a likely avenue to obtain such information. Care also needs to be taken in going that route, however, for two reasons. First, bond orders determined from force constants (or other methods) should usually be quite similar to those determined via the BVM, but the exact relationship is unclear, because different assumptions are associated

with each method. Second, we have seen that assuming the valence sum rule can lead to unexpected behavior such as the severe curvature noted in some of the bond valence-length curves in Fig. 4, and similar unexpected results may come from estimating bond order from force constants. We would expect the force constants for C–O bonds, for instance, to follow the traditional relationship of double and triple bonds having 2 and 3 times the force constant of a single bond, but this is not the case; e.g., CO (19.02 N/cm) is generally considered to have a triple bond, CO_2 (16.00 N/cm) to have double bonds, and CH_3OH (5.42 N/cm) to have a single C-O bond (Haynes, 2013). However, if we take methanol as the standard, CO_2 has nearly a triple C-O bond; or taking CO_2 as the standard, the methanol C-O bond has a bond order of only 5/8 and CO only about 2 1/3. Either way, we need to rethink simple Molecular Orbital assumptions about bonding for both crystals and molecules to relate them to the BVM.

Implications

Although it is probably not possible to relate ρ_b and bond valence in a quantitative manner, assuming at least a rough correspondence between the two has allowed us to draw out a striking implication. That is, the shape of the bond valence-length curve should change as a function of bond character (covalent, ionic, or metallic), with the curve becoming steeper in the high-valence range for more ionic and metallic bonds. This makes good chemical sense in terms of both the electronic structures of different types of atoms and the behavior of different types of bonds. We have, furthermore, shown that standard exponential and power-law forms of the bond valence-length relationship tend to systematically under-predict the bond valence of more ionic, high-valence bonds (1-2 v.u.) in oxide molecules, and that this behavior is consistent with our hypothesis. Crystals with

more ionic bonds tend not to exhibit such high-valence bonds, but our previous work (Bickmore et al., 2013) has demonstrated that this systematic under-prediction of bond valence could be a major problem even for bonds as weak as 0.25 v.u., in cases where very electropositive metals exhibit abnormally low coordination numbers.

These simple demonstrations show that, regardless of the true nature of the relationship between ρ_b and bond valence, a more flexible bond valence-distance curve shape (e.g., Eqn. 8) is needed for some purposes. While the standard exponential and power-law forms are probably adequate for modeling equilibrium geometries in most crystals, they will exhibit systematic deficiencies as their application broadens to include different bond types (O'Keeffe and Brese, 1992; Wander et al., in press) and non-equilibrium energy calculations (Adams and Swenson, 2002; Grinberg et al., 2002; Cooper et al., 2003; Shin et al., 2005; Adams and Rao, 2009; Grinberg et al., 2009; Liu et al., 2013a; Liu et al., 2013b).

We have also raised the possibility that the valence sum rule (Eqn. 3), and hence the concept of bond valence itself, is not really applicable to all the types of molecules examined here. Objections like these, however, would necessarily be rooted in attempts to rationalize bond valence in terms of particular physical concepts, such as electric flux between point charges, ρ_b, or some alternative method of estimating bond order. Given some precise definition of bond valence, one could argue that the variation in bond valence-length curve shape we have shown here indicates fundamental differences in the meaning of bonds having the same valence. For instance, a 2 v.u. bond in an MgO molecule might not "mean" the same thing as a 2 v.u. C=O bond in a formaldehyde (H_2CO) molecule.

While these attempts at rationalization are both useful and necessary, it should always be remembered that the true power of the BVM has always been in its empirical calibration, based on the enforcement of the valence sum rule for equilibrium geometries. This enforcement necessarily involves combining multiple phenomena under the bond-valence heading, including electrostatic interactions, Pauli repulsion, and Van der Waals interactions (Brown, 2002). And if so, the exact physical "meaning" of a given bond valence is *necessarily* dependent on the identities (i.e., electronic structures) of the bonded atoms.

Such variations are expected, and could actually be an asset for the model if they can be shown to be systematic. Here we have argued that the bond valence-length curve shape should vary systematically as a function of bond character, but it has long been known that other properties, such as the dissociation energies of bonds with the same nominal bond order, also vary quite strongly as a function of bond character (Pauling, 1960; Sanderson, 1983; Wander et al., in press).

Therefore, if we intend to expand the BVM to be capable of modeling more than equilibrium structures in condensed phases, it seems reasonable to keep the valence sum rule as the basis for determining bond valence, and then further explore systematic variations in bond properties as a function of bond valence in combination with other considerations such as bond character.

Acknowledgements

The authors would like to acknowledge support from the National Science Foundation Geobiology and Low-Temperature Geochemistry program (EAR-1227215), NASA (MFRP- NNX11AH11G), and the BYU College of Physical and Mathematical Sciences. We would also like to acknowledge stimulating conversations with Prof. I. David

Brown, Prof. G. V. Gibbs, and Olivier Gagne. Profs. Chérif Matta and I. David Brown

provided helpful reviews of the manuscript.

References

Adams, S. (2001) Relationship between bond valence and bond softness of alkali halides and chalcogenides. Acta Crystallographica, B57, 278-287.

Adams, S. and Swenson, J. (2002) Bond valence analysis of transport pathways in RMC models of fast ion conducting glasses. Physical Chemistry Chemical Physics, 4, 3179-3184.

Adams, S. and Rao, R.P. (2009) Transport pathways for mobile ions in disordered solids from the analysis of energy-scaled bond-valence mismatch landscapes. Physical Chemistry Chemical Physics, 11, 3210-3216.

Allred, A.L. (1961) Electronegativity values from thermochemical data. Journal of Inorganic and Nuclear Chemistry, 17, 215-221.

Almenningen, A., Bastiansen, O., Ewing, V., Hedberg, K., and Traetteberg, M. (1963) The molecular structure of disiloxane $(SiH_3)_2O$. Acta Chemica Scandinavica, 17, 2455-2460.

Bader, R. (1991) A quantum theory of molecular structure and its applications. Chemical Reviews, 91, 893-928.

Bader, R.F.W., Tang, T.H., Tal, Y., and Biegler-König, F.W. (1982) Molecular structure and its change: Hydrocarbons. Journal of the American Chemical Society, 104, 940-945.

Badger, R.M. (1934) A relation between internuclear distances and bond force constants. Journal of Chemical Physics, 2, 128-131.

Batsanov, S.S. and Batsanov, A.S. (2012) Introduction to Structural Chemistry, 542 p. Springer, Dordrecht.

Bickmore, B.R., Rosso, K.M., Brown, I.D., and Kerisit, S. (2009) Bond-valence constraints on liquid water structure. Journal of Physical Chemistry, A113, 1847-1857.

Bickmore, B.R., Wander, M.C.F., Edwards, J., Maurer, J., Shepherd, K., Meyer, E., Johansen, W.J., Frank, R.A., Andros, C., and Davis, M. (2013) Electronic structure effects in the vectorial bond-valence model. American Mineralogist, 98, 340-349.

Bolzan, A.A., Fong, C., Kennedy, B.J., and Howard, C.J. (1997) Structural studies of rutile-type metal dioxides. Acta Crystallographica B, 53, 373-380.

Brassington, N.J., Edwards, H.G.M., Long, D.A., and Skinner, M. (1978) The pure rotational Raman spectrum of SeO_3. Journal of Raman Spectroscopy, 7, 158-160.

Brown, I.D. (1981) The bond-valence method: An empirical approach to chemical structure and bonding. In M. O'Keefe and A. Navrotsky, Eds., Structure and Bonding in Crystals. Academic Press, New York.

Brown, I.D. (1988) What factors determine cation coordination numbers? Acta Crystallographica, B44, 545-553.

Brown, I.D. (2002) The Chemical Bond in Inorganic Chemistry: The bond valence model, 278 p. Oxford University Press, New York.

Brown, I.D. (2009) Recent developments in the methods and applications of the bond valence model. Chemical Reviews, 109, 6858-6919.

Brown, I.D. (2013) Bond valence theory. Structure and Bonding, DOI: 10.1007/430_2012_89.

Brown, I.D. and Shannon, R.D. (1973) Empirical bond-strength––bond-length curves for oxides. Acta Crystallographica, A29, 266-282.

Brown, I.D. and Altermatt, D. (1985) Bond-valence parameters obtained from a systematic analysis of the inorganic crystal structure database. Acta Crystallographica, B41, 244-247.

Brown, I.D. and Skowron, A. (1990) Electronegativity and Lewis acid strength. Journal of the American Chemical Society, 112, 3401-3403.

Burdett, J.K. and Hawthorne, F.C. (1993) An orbital approach to the theory of bond valence. American Mineralogist, 78, 884-892.

Cooper, V.R., Grinberg, I., and Rappe, A.M. (2003) Extending first principles modeling with crystal chemistry: A bond-valence based classical potential. In P.K. Davies and D.J. Singh, Eds., Fundamental Physics of Ferroelectrics. American Institute of Physics, Melville, New York.

Cotton, F.A. (1964) Ligand field theory. Journal of Chemical Education, 41, 466-476.

Cukrowski, I. and Matta, C.F. (2010) Hydrogen‐hydrogen bonding: A stabilizing interaction in strained chelating rings of metal complexes in aqueous phase. Chemical Physics Letters, 499, 66-69.

Darriet, B., Devalette, M., and Roulleau, F. (1974) Structure cristalline de K_6MgO_4. Acta Crystallographica B, 30, 2667-2669.

Firme, C.L., Antunes, O.A.C., and Esteves, P.M. (2009) Relation between bond order and delocalization index of QTAIM. Chemical Physics Letters, 468, 129–133.

Frisch, M.J., Trucks, G.W., Schlegel, H.B., Scuseria, G.E., Robb, M.A., Cheeseman, J.R., Montgomery, J., J. A. , Vreven, T., Kudin, K.N., Burant, J.C., Millam, J.M., Iyengar, S.S., Tomasi, J., Barone, V., Mennucci, B., Cossi, M., Scalmani, G., Rega, N., Petersson, G.A., Nakatsuji, H., Hada, M., Ehara, M., Toyota, K., Fukuda, R., Hasegawa, J., Ishida, M., Nakajima, T., Honda, Y., Kitao, O., Nakai, H., Klene, M., Li, X., Knox, J.E., Hratchian, H.P., Cross, J.B., Adamo, C., Jaramillo, J., Gomperts, R., Stratmann, R.E., Yazyev, O., Austin, A.J., Cammi, R., Pomelli, C., Ochterski, J.W., Ayala, P.Y., Morokuma, K., Voth, G.A., Salvador, P., Dannenberg, J.J., Zakrzewski, V.G., Dapprich, S., Daniels, A.D., Strain, M.C., Farkas, O., Malick, D.K., Rabuck, A.D., Raghavachari, K., Foresman, J.B., Ortiz, J.V., Cui, Q., Baboul, A.G., Clifford, S., Cioslowski, J., Stefanov, B.B., Liu, G., Liashenko, A., Piskorz, P., Komaromi, I., Martin, R.L., Fox, D.J., Keith, T., Al-Laham, M.A., Peng, C.Y., Nanayakkara, A., Challacombe, M., Gill, P.M.W., Johnson, B., Chen, W., Wong, M.W., Gonzalez, C., and Pople, J.A. (2010) Gaussian 09, p. Gaussian, Inc., Wallingford, CT.

Gibbs, G.V., Cox, D.F., and Rosso, K.M. (2004) A connection between empirical bond strength and the localization of the electron density at the bond critical points of the SiO bonds in silicates. Journal of Physical Chemistry, A108, 7643-7645.

Gibbs, G.V., Boisen, M.B., Beverly, L.L., and Rosso, K.M. (2001) A computational quantum chemical study of the bonded interactions in earth materials and structurally and chemically related molecules, Molecular Modeling Theory: Applications in the Geosciences.

Gibbs, G.V., Rosso, K.M., Cox, D.F., and Boisen Jr., M.B. (2003) A physical basis for Pauling's definition of bond strength. Physics and Chemistry of Minerals, 30, 317-320.

Gibbs, G.V., Ross, N.L., Cox, D.F., and Rosso, K.M. (2014) Insights into the crystal chemistry of earth materials rendered by electron density distributions: Pauling's rules revisted. American Mineralogist, 99.

Gibbs, G.V., Cox, D.F., Crawford, T.D., Rosso, K.M., Ross, N.L., and Downs, R.T. (2006) Classification of metal-oxide bonded interactions based on local potential- and kinetic-energy densities. Journal of Chemical Physics, 124.

Gibbs, G.V., Downs, R.T., Cox, D.F., Ross, N.L., Boisen Jr., M.B., and Rosso, K.M. (2008a) Shared and closed-shell O-O interactions in silicates. Journal of Physical Chemistry A, 112, 3693-3699.

Gibbs, G.V., Downs, R.T., Cox, D.F., Ross, N.L., Prewitt, C.T., Rosso, K.M., Lippmann, T., and Kirfel, A. (2008b) Bonded interactions and the crystal chemistry of minerals: A review. Zeitschrift fur Kristallographie, 223, 1-40.

Glidewell, C., Rankin, D.W.H., Robiette, A.G., Sheldrick, G.M., Beagley, B., and Cradock, S. (1970) Molecular structures of digermyl ether and digermyl sulphide in the gas phase, studied by electron diffraction. Journal of the Chemical Society A, 197, 315-317.

Grinberg, I., Cooper, V.R., and Rappe, A.M. (2002) Relationship between local structure and phase transitions of a disordered solid solution. Nature, 419, 909-911.

Grinberg, I., Shin, Y.-H., and Rappé, A.M. (2009) Molecular dynamics study of dielectric response in a relaxor ferroelectric. Physical Review Letters, 103, 197601.

Haaland, A. (2008) Molecules and Models: The Molecular Structures of Main Group Element Compounds, 304 p. Oxford, New York.

Haynes, W.M. (2013) Handbook of Chemistry and Physics. CRC Press, Boca Raton.

Hazen, R.M. (1976) Effects of temperature and pressure on the cell dimension and X-ray temperature factors of periclase. American Mineralogist, 61, 266-271.

Hazen, R.M. and Finger, L.W. (1986) High-pressure and high-temperature crystal chemistry of beryllium oxide. Journal of Applied Physics, 59, 3728-3733.

Jabłonski, M. and Palusiak, M. (2010) Basis Set and Method Dependence in Atoms in Molecules Calculations. Journal of Physical Chemistry A, 114, 2240–2244.

Johnston, V.H.S. (1966) Gas Phase Reaction Rate Theory, 372 p. Ronald Press, New York.

Keith, T.A. (2013) AIMAll (Version 13.11.04), p. TK Gristmill Software, Overland Park KS, USA.

Ketelaar (1958) Chemical Constitution: An Introduction to the Theory of the Chemical Bond, 398 p. Elsevier, Amsterdam.

Kihara, K. (1990) An X-ray study of the temperature dependence of the quartz structure. European Journal of Mineralogy, 2, 63-77.

Liu, S., Grinberg, I., and Rappé, A.M. (2013a) Development of a bond-valence based interatomic potential for BiFeO3 for accurate molecular dynamics simulations. Journal of Physics: Condensed Matter, 25, 102202.

Liu, S., Grinberg, I., Takenaka, H., and Rappé, A.M. (2013b) Reinterpretation of the bond-valence model with bond-order formalism: An improved bond-valence-based interatomic potential for $PbTiO_3$. Physical Review B, 88, 104102.

Matta, C.F. (2014) Modeling biophysical and biological properties from the characteristics of the molecular electron density, electron localization and delocalization matrices,

and the electrostatic potential. Journal of Computational Chemistry, 35, 1165–1198.

Matta, C.F. and Hernández–Trujillo, J. (2003) Bonding in polycyclic aromatic hydrocarbons in terms of the the electron density and of electron delocalization. Journal of Physical Chemistry A, 107, 7496–7504.

O'Keeffe, M. and Brese, N.E. (1992) Bond-valence parameters for anion-anion bonds in solids. Acta Crystallographica, B48, 152-154.

Pauling, L. (1947) Atomic radii and interatomic distances in metals. Journal of the American Chemical Society, 69, 542-553.

Pauling, L. (1960) The Nature of the Chemical Bond, 644 p. Cornell University Press, Ithaca.

Popelier, P.L.A. (2000) Atoms in Molecules: An Introduction, 164 p. Pearson Education, Essex.

Preiser, C., Lösel, J., Brown, I.D., Kunz, M., and Skowron, A. (1999) Long-range Coulomb forces and localized bonds. Acta Crystallographica, B55, 698-711.

Rzepa, H.S. (2009) The importance of being bonded. Nature Chemistry, 1, 510-512.

Sanderson, R.T. (1983) Polar Covalence, 240 p. Academic Press, New York.

Schuldt, D. and Hoppe, R. (1989) Zum Aufbau von $RbNa_5Be_8O_{11}$. Zeitschrift für Anorganische und Allgemeine Chemie, 575, 77-89.

Shin, Y.-H., Cooper, V.R., Grinberg, I., and Rappe, A.M. (2005) Development of a bond-valence molecular-dynamics model for complex oxides. Physical Review B, 71, No. 054104.

Smyth, J.R., Swope, R.J., and Pawley, A.R. (1995) H in rutile-type compounds: II. Crystal chemistry of Al substitution in H-bearing stishovite. American Mineralogist, 80, 454-456.

Wander, M.C.F., Bickmore, B.R., Davis, M., Johansen, W.J., Andros, C., and Lind, L. (in press) The use of cation-cation and anion-anion bonds to augment the bond-valence model. American Mineralogist.

Yamanaka, T. and Ogata, K. (1991) Structure refinement of GeO2 polymorphs at high pressures and temperatures by energy-dispersive spectra of powder diffraction. Journal of Applied Crystallography, 24, 111-118.

Zhurova, E.A., Matta, C.F., Wu, N., Zhurov, V.V., and Pinkerton, A.A. (2006) Experimental and theoretical electron density study of estrone. Journal of the American Chemical Society, 128, 8849–8861.

Table 1. Calculated ρ_b values in $e^-/Å^3$ for all the diatomic pairs at various interatomic distances. The ρ_b values for a few elements could not be calculated at 6 Å because the electron density profile was too weak to form a saddle point. In essence, the atoms are completely unbound. The ρ_b value for the HF pair at 0.5 Å could not be calculated, because The ρ_b has only one maximum corresponding to the region around the F nucleus.

		Distance (Å)								
Atom1	**Atom 2**	**0.5**	**1**	**1.5**	**2**	**2.5**	**3**	**3.5**	**4**	**6**
Li	Li	1.13E+01	1.11E+00	1.57E-01	1.23E-01	1.05E-01	7.76E-02	5.40E-02	3.60E-02	4.66E-03
Li	Be	1.22E+01	8.92E-01	3.04E-01	2.46E-01	1.25E-01	6.41E-02	3.76E-02	2.28E-02	2.32E-03
Li	B	1.22E+01	8.56E-01	4.52E-01	3.04E-01	1.42E-01	7.63E-02	4.74E-02	3.13E-02	3.01E-03
Li	H	3.68E+00	9.63E-01	3.27E-01	1.40E-01	7.33E-02	4.64E-02	3.21E-02	1.67E-02	8.95E-04
Li	C	1.29E+01	1.14E+00	4.69E-01	2.92E-01	1.26E-01	6.68E-02	3.27E-02	1.45E-02	1.48E-03
Li	N	1.41E+01	2.64E+00	8.11E-01	2.62E-01	1.07E-01	5.09E-02	2.82E-02	1.44E-02	1.01E-03
Li	O	1.51E+01	2.74E+00	7.38E-01	2.17E-01	8.26E-02	4.30E-02	2.49E-02	1.91E-02	
Li	F	1.81E+01	3.19E+00	6.56E-01	1.73E-01	5.71E-02	2.20E-02	9.20E-03	4.08E-03	2.63E-04
Be	Be	1.23E+01	7.08E-01	5.76E-01	4.27E-01	2.10E-01	9.88E-02	4.72E-02	2.31E-02	1.26E-03
Be	B	1.20E+01	1.02E+00	3.66E-01	3.66E-01	1.94E-01	8.32E-02	5.25E-02	2.52E-02	1.34E-03
Be	H	4.89E+00	1.28E+00	5.02E-01	2.60E-01	1.12E-01	4.42E-02	1.91E-02	8.40E-03	3.11E-04
Be	C	1.20E+01	2.33E+00	8.23E-01	3.28E-01	1.78E-01	7.21E-02	2.87E-02	1.16E-02	7.07E-04
Be	N	1.22E+01	2.89E+00	9.51E-01	3.62E-01	1.65E-01	6.68E-02	2.85E-02	1.23E-02	3.99E-04
Be	O	1.30E+01	3.34E+00	7.56E-01	2.42E-01	1.43E-01	6.20E-02	2.13E-02	1.21E-02	3.73E-04
Be	F	1.88E+01	3.35E+00	7.09E-01	2.33E-01	1.33E-01	8.02E-02	2.16E-02	2.27E-02	5.49E-04
B	B	1.12E+01	2.61E+00	1.14E+00	6.19E-01	2.73E-01	1.24E-01	5.85E-02	2.76E-02	1.43E-03
B	H	6.70E+00	1.89E+00	8.30E-01	3.65E-01	1.63E-01	7.12E-02	2.94E-02	1.16E-02	3.32E-04
B	C	1.06E+01	2.58E+00	1.52E+00	7.20E-01	3.25E-01	1.23E-01	4.89E-02	2.04E-02	2.87E-04
B	N	1.07E+01	3.31E+00	1.21E+00	4.45E-01	2.66E-01	9.12E-02	3.70E-02	1.35E-02	1.36E-04
B	O	1.47E+01	3.80E+00	1.12E+00	4.06E-01	1.26E-01	3.79E-02	1.31E-02	4.63E-03	1.44E-04
B	F	2.35E+01	3.74E+00	9.13E-01	4.26E-01	1.87E-01	8.47E-02	4.17E-02	2.04E-02	
H	H	3.47E+00	1.02E+00	3.79E-01	1.38E-01	4.79E-02	1.69E-02	6.08E-03	2.27E-03	5.54E-05
H	C	8.32E+00	2.49E+00	8.59E-01	3.35E-01	1.08E-01	3.75E-02	1.32E-02	5.36E-03	1.42E-04

H	N	1.03E+01	2.51E+00	7.88E-01	2.48E-01	7.65E-02	2.60E-02	9.23E-03	3.40E-03	6.16E-05
H	O	1.18E+01	2.31E+00	7.05E-01	2.12E-01	6.03E-02	1.93E-02	9.94E-03	3.79E-03	3.04E-05
H	F		2.04E+00	6.22E-01	2.21E-01	6.87E-02	2.07E-02	6.61E-03	2.20E-03	2.87E-05
C	C	8.94E+00	3.72E+00	1.90E+00	7.21E-01	2.82E-01	1.00E-01	3.39E-02	1.18E-02	2.24E-04
C	N	1.30E+01	4.46E+00	1.80E+00	6.42E-01	2.11E-01	6.70E-02	2.32E-02	8.71E-03	5.61E-05
C	O	2.15E+01	4.81E+00	1.63E+00	5.63E-01	1.94E-01	5.94E-02	1.79E-02	5.83E-03	9.33E-05
C	F	2.75E+01	4.36E+00	1.33E+00	5.09E-01	1.85E-01	3.82E-02	7.20E-04	4.76E-03	6.23E-05
N	N	2.08E+01	6.16E+00	1.83E+00	5.81E-01	1.09E-01	3.08E-02	9.25E-03	2.84E-03	
N	O	2.68E+01	5.94E+00	1.74E+00	4.91E-01	8.13E-02	3.60E-02	1.09E-02	3.76E-03	7.80E-05
N	F	1.07E+01	3.31E+00	1.21E+00	4.45E-01	2.66E-01	9.12E-02	3.70E-02	1.35E-02	1.36E-04
O	O	3.19E+01	6.68E+00	1.69E+00	4.91E-01	1.40E-01	2.79E-02	5.55E-03	1.15E-03	
O	F	3.60E+01	6.44E+00	1.57E+00	3.59E-01	7.76E-02	1.91E-02	8.43E-03	2.67E-03	1.56E-05
F	F	4.03E+01	6.83E+00	1.49E+00	3.55E-01	7.72E-02	1.75E-02	4.59E-03	1.19E-03	

688 **Table 2.** Summary of ρ_b-distance model fits for the exponential (Eqn. 1), power-law (Eqn. 2), three-parameter hybrid (Eqn. 5),
689 and four-parameter hybrid (Eqn. 6) forms. The sum of squared error is also reported for all three models.

		Exponential		*Power*		*Hybrid*			Residual			
Atom 1	**Atom 2**	***B***	***R_0***	***B***	***R_0***	***w***	***B***	***R_0***	**Exp.**	**Power**	**Hybrid-3**	**Hybrid-4**
Li	Li	0.8480	0.9866	0.3564	1.0567	0.0069	0.3590	1.0578	1.20E+00	3.99E-01	4.15E-01	4.15E-01
Li	Be	0.7312	1.1910	0.3212	1.1197	0.1806	0.3833	1.1608	1.20E+00	7.03E-02	4.95E-01	4.95E-01
Li	B	0.7548	1.2841	0.3335	1.1622	0.2093	0.4082	1.2196	1.17E+00	1.03E-01	5.12E-01	5.12E-01
Li	H	0.7088	0.9294	0.3268	0.9612	0.4778	0.4939	0.9834	2.31E-01	4.64E-01	5.23E-02	5.23E-02
Li	C	0.6601	1.3286	0.2958	1.1756	0.2840	0.3857	1.2568	1.18E+00	6.36E-01	4.20E-01	4.20E-01
Li	N	0.5979	1.4807	0.2694	1.2547	0.3179	0.3611	1.3706	1.12E+00	2.04E+00	4.77E-02	4.77E-02
Li	O	0.5269	1.4992	0.2958	1.2349	0.1463	0.3247	1.2903	1.21E+00	8.87E-01	3.18E-01	3.18E-01
Li	F	0.4993	1.3776	0.2240	1.2008	0.2912	0.2938	1.2917	1.54E+00	3.99E+00	4.50E-01	4.50E-01
Be	Be	0.6770	1.4171	0.3129	1.2017	0.4993	0.4802	1.3524	1.06E+00	5.44E-01	6.98E-01	6.98E-01
Be	B	0.6856	1.3814	0.3134	1.1898	0.4126	0.4518	1.3116	1.06E+00	4.94E-01	5.95E-01	5.95E-01
Be	H	0.5836	1.2190	0.2772	1.0764	0.7709	0.5060	1.2085	1.84E-01	1.38E+00	6.86E-02	6.86E-02
Be	C	0.5824	1.5282	0.2697	1.2637	0.5155	0.4186	1.4474	7.67E-01	2.39E+00	1.29E-01	1.29E-01
Be	N	0.5480	1.5829	0.2572	1.2875	0.6379	0.4328	1.5195	6.23E-01	3.42E+00	1.03E-01	1.03E-01
Be	O	0.5437	1.5302	0.2521	1.2639	0.5272	0.3944	1.4514	7.95E-01	3.33E+00	6.74E-02	6.74E-02
Be	F	0.5641	1.5807	0.2571	1.3052	0.3924	0.3651	1.4640	1.51E+00	2.87E+00	2.52E-01	2.52E-01
B	B	0.6366	1.7233	0.2995	1.3735	0.6659	0.5131	1.6542	5.50E-01	2.25E+00	1.99E-01	1.99E-01
B	H	0.5685	1.4602	0.2730	1.1995	0.9138	0.5400	1.4492	1.67E-01	2.25E+00	1.10E-01	1.10E-01
B	C	0.5427	1.7687	0.2663	1.3780	1.0000	0.5427	1.7687	1.97E-01	4.30E+00	1.97E-01	3.68E-01
B	N	0.5049	1.6971	0.2469	1.3327	1.0000	0.5049	1.6971	9.15E-02	5.29E+00	9.15E-02	2.63E-01
B	O	0.4733	1.5797	0.2224	1.2845	0.6538	0.3781	1.5198	6.19E-01	6.85E+00	1.78E-01	1.78E-01
B	F	0.5265	1.7442	0.2991	1.4122	0.2513	0.3493	1.5306	1.84E+00	1.25E+00	6.35E-02	6.35E-02
H	H	0.4981	1.0174	0.2376	0.9750	0.8216	0.4465	1.0268	8.03E-02	1.65E+00	8.09E-03	8.09E-03
H	C	0.4997	1.4378	0.2374	1.1941	0.7742	0.4342	1.4094	2.23E-01	3.85E+00	4.56E-02	4.56E-02
H	N	0.4604	1.4050	0.2178	1.1785	0.7262	0.3872	1.3730	3.92E-01	5.12E+00	2.96E-02	2.96E-02
H	O	0.4414	1.3946	0.2094	1.1708	0.7583	0.3794	1.3675	5.32E-01	5.79E+00	1.40E-01	1.40E-01
H	F	0.4462	1.2964	0.1661	1.3938	0.8973	0.4161	1.3089	8.51E-01	6.84E+01	1.04E+00	6.85E-03
C	C	0.5137	1.7546	0.2523	1.3680	1.0000	0.5137	1.7546	3.31E-01	5.64E+00	3.31E-01	6.98E-02

C	N	0.4495	1.7504	0.2207	1.3652	1.0000	0.4495	1.7504	4.06E-01	1.02E+01	4.06E-01	1.75E-01
C	O	0.4486	1.7516	0.2141	1.3834	0.8296	0.4043	1.7180	6.61E-01	1.18E+01	1.57E-01	1.57E-01
C	F	0.4124	1.6210	0.1922	1.3152	0.5698	0.3094	1.5391	1.54E+00	1.57E+01	6.13E-01	6.13E-01
N	N	0.3863	1.7027	0.2321	1.3547	1.0000	0.3863	1.7027	2.43E-01	7.51E+00	2.43E-01	7.06E-02
N	O	0.4284	1.6917	0.2003	1.3571	0.6028	0.3296	1.6100	1.34E+00	1.49E+01	5.55E-01	5.55E-01
N	F	0.5049	1.6971	0.2469	1.3327	1.0000	0.5049	1.6971	9.15E-02	5.29E+00	9.15E-02	2.63E-01
O	O	0.3481	1.7132	0.2098	1.3619	1.0000	0.3481	1.7132	1.87E-01	1.24E+01	1.87E-01	4.98E-01
O	F	0.3810	1.6760	0.1798	1.3414	0.6981	0.3142	1.6176	1.76E+00	2.57E+01	1.30E-01	1.30E-01
F	F	0.3377	1.6700	0.2002	1.3344	0.8052	0.3081	1.6279	1.20E+00	1.35E+01	3.34E-02	3.34E-02

690

691

692

693

Table 3. Three-parameter (Eqn. 5) and four-parameter (Eqn. 6) hybrid weighting factors (*w*). A value of 1 would indicate a pure exponential form, while a value of 0 would indicate a pure power-law form. Boxes bound metals, metalloids, and nonmetals. Light grey shading indicates non-polar covalent bonding, medium gray indicates polar covalent bonding, and dark grey indicates ionic bonding.

Hybrid - 3

	Li	Be	B	H	C	N	O	F
Li	0.0069	x	x	x	x	x	x	x
Be	0.1806	0.4993	x	x	x	x	x	x
B	0.2093	0.4126	0.6659	x	x	x	x	x
H	0.4778	0.7709	0.9138	0.8216	x	x	x	x
C	0.2840	0.5155	1.0000	0.7742	1.0000	x	x	x
N	0.3179	0.6379	1.0000	0.7262	1.0000	1.0000	x	x
O	0.1463	0.5272	0.6538	0.7583	0.8296	0.6028	1.0000	x
F	0.2912	0.3924	0.2513	0.8973	0.5698	1.0000	0.6981	0.8052

694

695

696 **Table 4.** Bond lengths for a number of oxo-molecules, from structures obtained either experimentally or via quantum
697 mechanical calculations. (The molecular formulas for which we obtained experimental values are bolded and italicized.) All of
698 these bonds should have bond valences of either ~1 v.u., or ~2 v.u. We also report bond valences calculated for these bond
699 lengths using Eqn. 1 and R_0 and B parameters obtained from either Brown and Altermatt (1985), or the SoftBV parameters of
700 Adams (2001). Finally, we report bond valences calculated for these bond lengths using two power-law forms similar to Eqn.
701 2 and associated parameters proposed by Brown and Shannon (1973). One form is meant for individual X-O pairs, and the
702 other is a "universal" model, where the parameters are the same for all X-O bonds for which X has the same number of core
703 electrons.

Molecule	Bond	$R_{X\text{-}O}$ (Å)	s_{ij} (v.u.)†	s_{ij} (v.u.)‡	s_{ij} (v.u.)*	s_{ij} (v.u.)#
H_2O	H-O	0.958	0.815	0.826	0.797	0.791
Li_2O	Li-O	1.606	0.686	0.430	0.537	0.537
K_2O	K-O	2.260	0.708	0.481	0.387	0.360
Na_2O	Na-O	1.979	0.622	0.421	0.547	0.426
LiOH	Li-O	1.582	0.732	0.451	0.570	0.571
LiOH	H-O	0.969	0.791	0.806	0.777	0.772
NaOH	Na-O	1.950	0.673	0.428	0.595	0.454
NaOH	H-O	0.941	0.852	0.856	0.828	0.822
KOH	K-O	2.223	0.782	0.523	0.420	0.387
KOH	H-O	0.957	0.816	0.827	0.798	0.792
$O(BeH)_2$	Be-O	1.407	0.932	0.635	0.963	0.918
$O(BH_2)_2$	B-O	1.368	1.008	0.992	1.019	1.029
$O(CH_3)_2$	C-O	1.410	0.948	0.974		
$O(SiH_3)_2$[b]	Si-O	1.634	0.974	0.942	0.975	0.969
$O(GeH_3)_2$[c]	Ge-O	1.766	0.953	0.935	0.952	0.933
OH(BeH)	Be-O	1.406	0.935	0.694	0.966	0.921
OH(BeH)	H-O	0.952	0.828	0.837	0.808	0.802
$OH(BH_2)$	B-O	1.366	1.014	0.994	1.027	1.037
$OH(BH_2)$	H-O	0.967	0.796	0.81	0.781	0.776
$OH(CH_3)$	C-O	1.422	0.918	0.949		
$OH(CH_3)$	H-O	0.962	0.806	0.819	0.790	0.784

$OH(MgH)$	Mg-O	1.765	0.824	0.578	0.790	0.696
$OH(MgH)$	H-O	0.949	0.834	0.841	0.813	0.807
$OH(AlH_2)$	Al-O	1.700	0.876	0.788	0.892	0.817
$OH(AlH_2)$	H-O	0.958	0.815	0.825	0.796	0.791
$OH(SiH_3)$	Si-O	1.653	0.925	0.973	0.926	0.922
$OH(SiH_3)$	H-O	0.960	0.811	0.822	0.793	0.788
$OH(CaH)$	Ca-O	2.011	0.888	0.635	0.854	0.607
$OH(CaH)$	H-O	0.956	0.820	0.830	0.801	0.795
$OH(ScH_2)$	Sc-O	1.851	0.995	0.787	1.133	0.881
$OH(ScH_2)$	H-O	0.956	0.819	0.829	0.800	0.795
$OH(TiH_3)$	Ti-O	1.751	1.190	0.948	1.029	1.129
$OH(TiH_3)$	H-O	0.957	0.817	0.827	0.798	0.792
$OH(GeH_3)$	Ge-O	1.795	0.881	0.869	0.871	0.845
$OH(GeH_3)$	H-O	0.962	0.806	0.818	0.789	0.784
$O(BH_2)(AlH_2)$	B-O	1.336	1.099	1.016	1.118	1.134
$O(BH_2)(AlH_2)$	Al-O	1.690	0.900	0.806	0.919	0.838
$O(BH_2)(SiH_3)$	B-O	1.350	1.059	1.006	1.074	1.087
$O(BH_2)(SiH_3)$	Si-O	1.665	0.897	0.966	0,898	0.895
$O(BH_2)(ZnH)$	B-O	1.330	1.117	1.020	1.138	1.138
$O(BH_2)(ZnH)$	Zn-O	1.766	0.846	0.934	0.814	0.932
$O(BH_2)(GaH_2)$	B-O	1.345	1.073	1.009	1.09	1.104
$O(BH_2)(GaH_2)$	Ga-O	1.822	0.781	0.753	0.781	0.774
$O(BH_2)(CdH)$	B-O	1.326	1.130	1.024	1.153	1.170
$O(BH_2)(CdH)$	Cd-O	1.964	0.852	0.736		
$O(CH_3)(BH_2)$	C-O	1.431	0.897	0.930		
$O(CH_3)(BH_2)$	B-O	1.343	1.079	1.039	1.096	1.110
$O(AlH_2)(SiH_3)$	Al-O	1.687	0.909	0.813	0.929	0.846
$O(AlH_2)(SiH_3)$	Si-O	1.623	0.987	0.987	0.990	0.982
$O(SiH_3)(GeH_3)$	Si-O	1.636	0.968	0.983	0.97	0.964
$O(SiH_3)(GeH_3)$	Ge-O	1.785	0.905	0.891	0.899	0.875
$\boldsymbol{HOCH_2OOH}$	C-O	1.385	1.015	1.031		
$\boldsymbol{HOCH_2OOH}$	H-O	0.965	0.800	0.814	0.785	

BeO	Be=O	1.331	1.145	0.798	1.152	1.152
HBO	B=O	1.200	1.588	1.506	1.755	1.755
B_2O_2[a]	B=O	1.198	1.595	1.513	1.765	1.765
CO_2	C=O	1.162	1.852	1.696		
MgO	Mg=O	1.749	0.860	0.596	0.724	0.724
CaO	Ca=O	1.822	1.479	0.945	0.607	0.607
HAlO	Al=O	1.598	1.155	1.002	1.217	1.066
SiO_2	Si=O	1.510	1.360	1.254	1.358	1.358
H_3PO	P=O	1.478	1.457	1.385	1.491	1.491
SO_3	S=O	1.418	1.748	1.664	1.783	1.783
HScO	Sc=O	1.673	1.609	1.127	2.076	1.385
TiO_2	Ti=O	1.706	1.345	1.037	1.270	1.270
ZnO	Zn=O	1.713	0.976	0.862	1.122	1.122
HGaO	Ga=O	1.648	1.247	1.199	1.262	1.417
GeO_2	Ge=O	1.624	1.399	1.338	1.549	1.549
SeO_3[d]	Se=O	1.688	1.312	1.305		
SrO	Sr=O	1.936	1.634	1.038		
ZrO_2	Zr=O	1.857	1.210	0.975		
CdO	Cd=O	1.909	0.986	0.842		
SnO_2	Sn=O	1.813	1.283	1.227		
BaO	Ba=O	1.996	2.187	1.456		
HfO_2	Hf=O	1.866	1.167	0.935		
HgO	Hg=O	1.913	1.172	0.805		
PbO_2	Pb=O	1.887	1.145	1.509		

† Exponential with parameters taken from Brown and Altermatt (1985).
‡ Exponential with parameters taken from Adams (2001).
* Power-law with parameters for individual bond types taken from Brown and Shannon (1973).
# Power-law with "universal" parameters taken from Brown and Shannon (1973).
[a] Bond-valence parameters for B^{3+} were used.
[b, c, d] Experimental structures taken from Almenningen et al. (1963), Glidewell et al. (1970), and Brassington et al. (1978), respectively. Otherwise, experimental structures were taken from the NIST Computational Chemistry Comparison and Benchmark Database (http://cccbdb.nist.gov).

Table 5. Crystal structures chosen for model fits of four bond types. For each bond type, two crystal structures were chosen that had two different cation coordination numbers and very symmetrical cation coordination polyhedra (variations in bond lengths no more than a few hundredths of an Å). Thus, an average bond length could be accurately associated with the average (assumed) bond valence (the cation valence divided by the coordination number).

Bond	Crystal	$R_{M\text{-}O}$ (avg.)	s_{ij} (assumed)	Source
Mg-O	MgO (Periclase)	2.112	0.333	(Hazen, 1976)
Mg-O	K_6MgO_4	2.024	0.5	(Darriet et al., 1974)
Be-O	BeO (Bromellite)	1.651	0.5	(Hazen and Finger, 1986)
Be-O	$RbNa_5Be_8O_{11}$	1.5603	0.667	(Schuldt and Hoppe, 1989)
Si-O	SiO_2 (α-Quartz)	1.609	1.000	(Kihara, 1990)
Si-O	SiO_2 (Stishovite)	1.758	0.667	(Smyth et al., 1995)
Ge-O	GeO_2 (quartz-like)	1.739	1.000	(Yamanaka and Ogata, 1991)
Ge-O	GeO_2 (Argutite)	1.888	0.667	(Bolzan et al., 1997)

Table 6. Summary of BV-distance model fits for the oxides in figure 4: three-parameter geometric hybrid (Eqn. 5), and four-parameter arithmetic hybrid (Eqn. 8) forms. The sum of squared error is also reported for both models.

		Hybrid Geometric			*Hybrid Arithmetic*				*Residual*	
Atom 1	**Atom 2**	***w***	***B***	R_0	***w***	***Be***	***Bp***	R_0	**Hyb-G3**	**Hyb-A4**
Mg	O	0.0000	0.1122	1.8428	0.0029	0.0029	0.1790	1.7659	0.3912	0.0023
Be	O	0.0000	0.1355	1.4504	0.0018	0.0129	0.2388	1.4086	0.0954	0.0005
Si	O	0.0000	0.1184	1.6344	0.0002	0.0140	0.2103	1.6196	0.0383	0.0028
Ge	O	0.0000	0.1273	1.7698	0.0001	0.0144	0.2038	1.7554	0.0315	0.0095

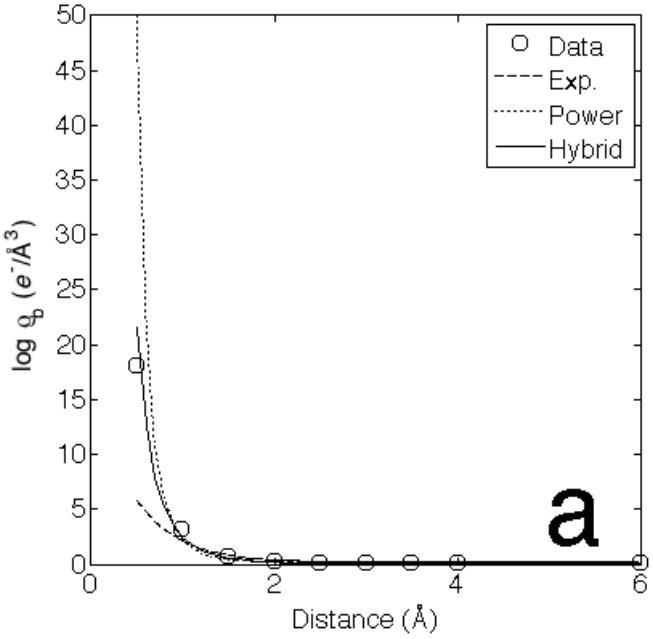

716

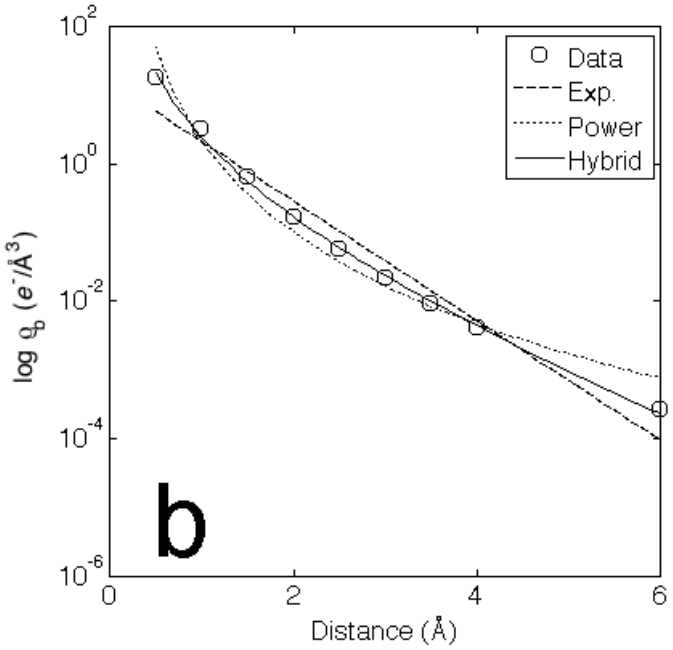

Figure 1. Electron density profile for the Li-F scan illustrated with two types of plot: (a) linear-linear plot, and (b) log-linear. Best-fit lines for the exponential (Eqn. 1) and power-law (Eqn. 2) forms of the bond-valence equation are also shown. The linear-linear plot is useful for looking at the difference in fit between the functional forms for very short bonds (e.g., that one might find in transition states,) while the log-linear plot is useful for comparing the relative quality of the fit across the sampled range.

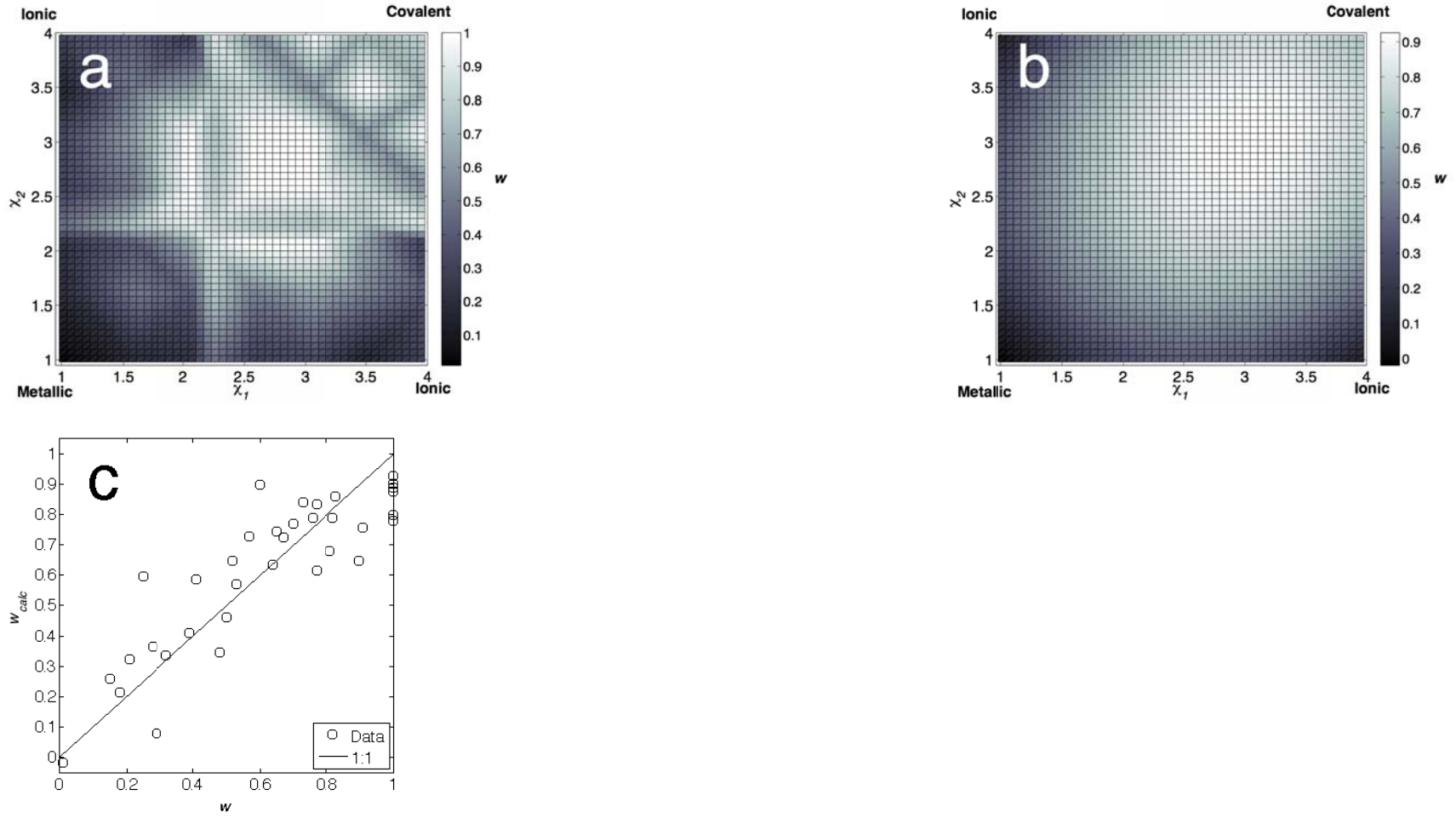

Figure 2. (a) Interpolated contour plot of the weighting factor (w) in the three-parameter hybrid model (Eqn. 5) for the Row 1 and 2 diatomic molecules. The shading indicates the w value (see Table 3), and the two axes represent the Pauling electronegativities of the two atoms (χ_1 and χ_2). The corners are labeled to show where the most ionic, covalent, and metallic atoms would be. (b) Instead of interpolating, we fit a second-order polynomial to the data, shown here. (c) Plot of the weighting factor calculated via the second-order polynomial (w_{calc}) vs. that taken from Table 3 (w).

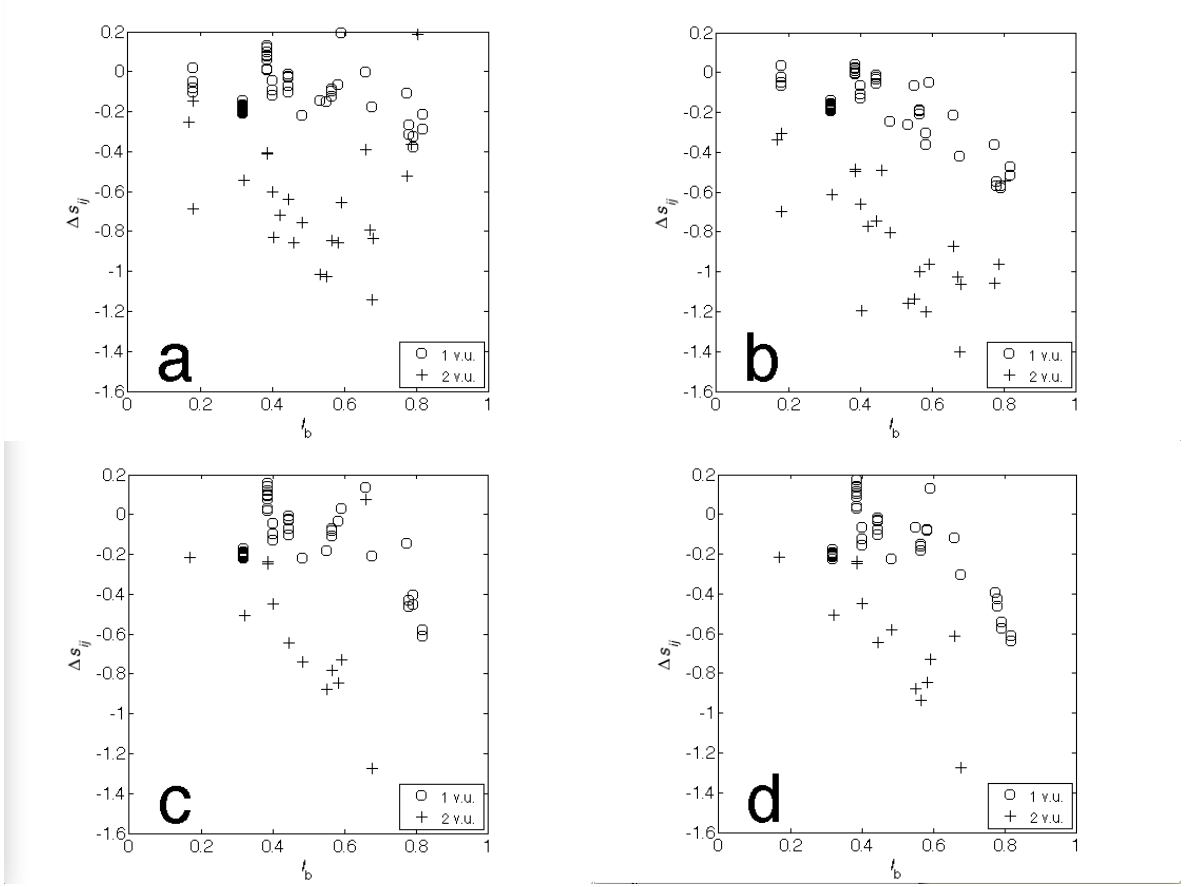

Figure 3. The difference (Δs_{ij}) between calculated X-O bond valences and the inferred bond valences (~1 v.u. or ~2 v.u.) for the molecules listed in Table 4, plotted vs. the Pauling fraction ionic character of the bonds (I_b), calculated as $I_b = 1 - e^{-0.25(\chi_A - \chi_B)^2}$ (Pauling, 1960), where χ_A and χ_B are the Pauling electronegativity values of the two atoms. Bond valence values were calculated using Eqn. 1 (the exponential form) and R_0 and B parameters obtained from either (a) Brown and Altermatt (1985), for which B is always set to 0.37 Å, or (b) the SoftBV parameters of Adams (2001), which have various B values. Bond valences were also calculated using two power-law forms and associated parameters proposed by Brown and Shannon (1973), including (c) a form meant for individual X-O pairs and (d) another "universal" model, where the parameters are the same for all X-O bonds for which X has the same number of core electrons.

744
745

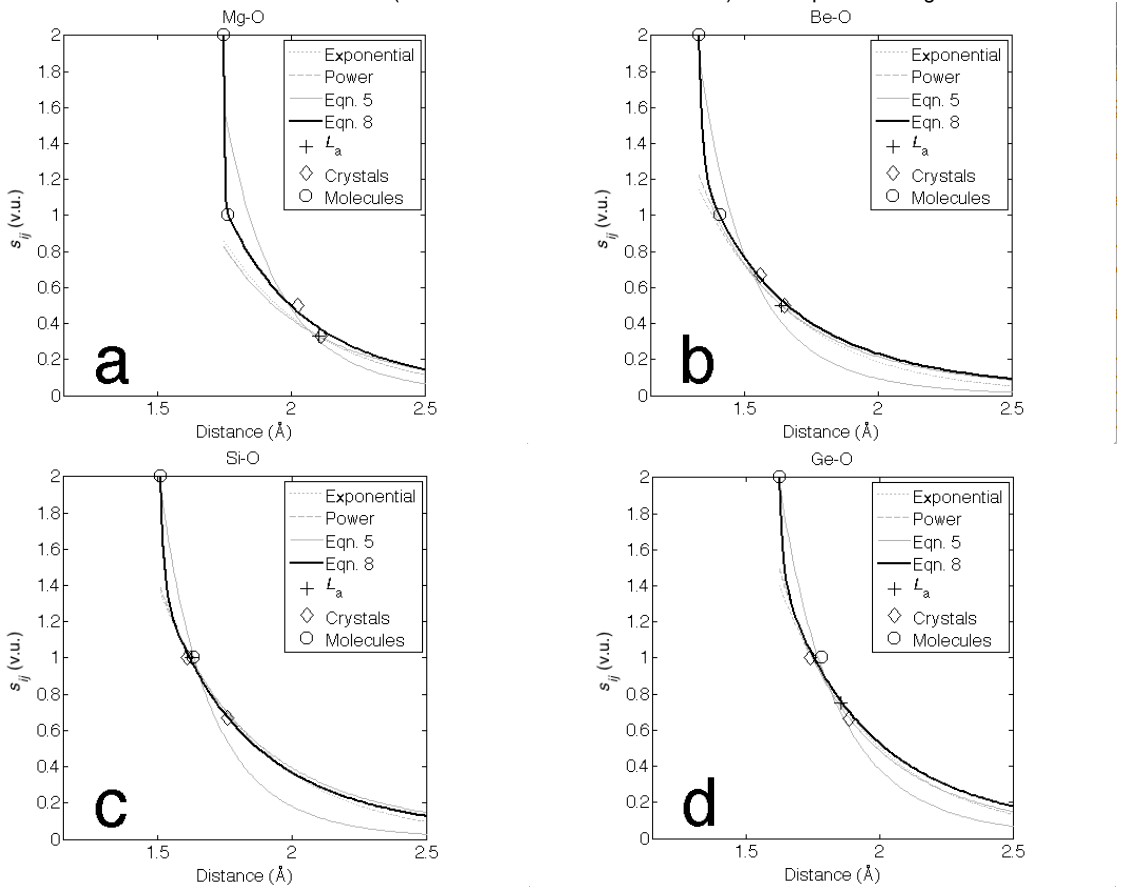

Figure 4. Bond valence (s_{ij}) vs. bond length (R) for four bond types involving Oxygen with varying fraction ionic character (I_b): (a) Mg-O (I_b = 0.68), (b) Be-O (I_b = 0.58), (c) Si-O (I_b = 0.45), and (d) Ge-O (I_b = 0.40). For each bond type, we show points representing the 1 and 2 v.u. bond lengths from molecules in Table 4 (circles), the Lewis acid strength ($L_{A,X}$) value with the corresponding bond length calculated using Eqn. 1 and Brown and Altermatt's (1985) parameters (crosses), and two bond lengths from crystals corresponding to easily estimated bond valances from different cation coordination numbers (diamonds). The grey dashed and dotted lines denote the exponential and power-law bond valence-length curves (Brown and

757 Shannon, 1973; Brown and Altermatt, 1985), respectively. The grey solid line represents a fit of Eqn. 5 to the molecule and
758 crystal points, whereas the thicker, black solid line represents a fit of Eqn. 8.
759

760

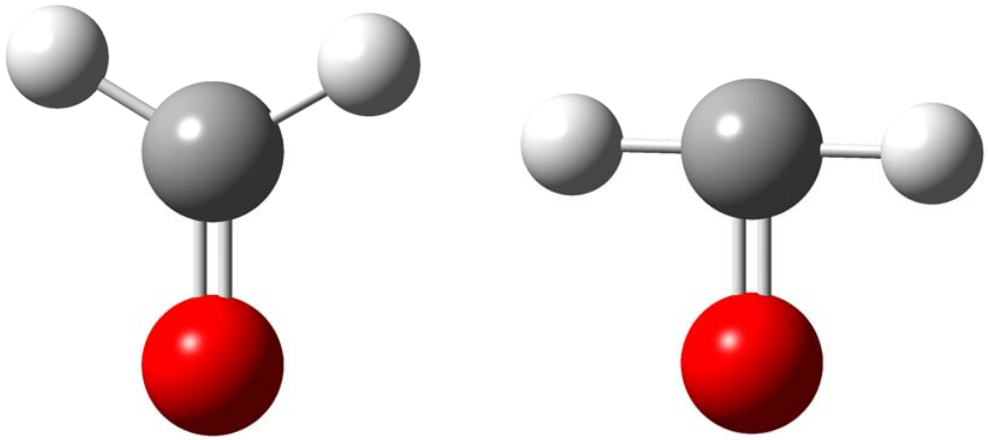

761
762 **Schema 1.** While the molecule on the left (H_2CO) will have the same bond valence for both CO and CH bonds according to the
763 BVM, AIM analysis will show different ρ_b values for the bonds, even though all pair distances are unchanged.
764
765

766 Supplemental Materials
767
768

Table S1. Spin States used for calculations. Wherever possible spin states were taken from NIST's Computational Chemistry Comparison and Benchmark DataBase. The remaining few were decided from molecular orbital considerations.

Atom1	Atom2	Spin
H	H	1
H	Li	1
H	Be	2
H	B	1
H	C	2
H	N	3
H	O	2
H	F	1
Li	Li	1
Li	Be	2
Li	B	1
Li	C	2
Li	N	3
Li	O	2
Li	F	1
Be	Be	1
Be	B	2
Be	C	3
Be	N	4
Be	O	1
Be	F	2
B	B	3
B	C	2
B	N	3
B	O	2

B	F	1
C	C	1
C	N	2
C	O	1
C	F	2
N	N	0
N	O	2
N	F	3
O	O	3
O	F	2
F	F	1
Al	H	1
Al	O	2
Si	H	2
Si	O	1
Al	Si	2
Si	Si	3
Al	Al	3

769